The interaction of growth with mechanical constraints drives puzzle cell formation in plants

Nicola Trozzi[1,2,3], Brendan Lane[1], Alice Perruchoud[2], Frances Clark[4], Lukas Hoermayer[2], Andrea Meraviglia[2], Tammo Reichgelt[5], Adrienne H.K. Roeder[4], Dorota Kwiatkowska[6], Adam Runions[7], Richard S. Smith[1]✉ and Mateusz Majda[1,2]✉

[1]Department of Computational and Systems Biology, John Innes Centre, Norwich NR4 7UH, UK.
[2]Department of Plant Molecular Biology, University of Lausanne, CH-1015 Lausanne, Switzerland.
[3]School of Biological Sciences, University of East Anglia, Norwich, NR4 7TJ UK
[4]Weill Institute for Cell and Molecular Biology and School of Integrative Plant Science, Section of Plant Biology, Cornell University, Ithaca, NY 14853, USA.
[5]Department of Earth Sciences, University of Connecticut, Beach Hall, 354 Mansfield Rd, Storrs CT 06269, USA.
[6]Institute of Biology, Biotechnology and Environmental Protection, Faculty of Natural Sciences, University of Silesia, 40-032 Katowice, Poland.
[7]Department of Computer Science, University of Calgary, Calgary, AB T2N 1N4, Canada.
✉To whom correspondence may be addressed: Mateusz.Majda@unil.ch, Richard.Smith@jic.ac.uk.

Abstract

Plant cells often develop shapes that mirror the overall morphology of their organs. This relationship suggests that cell shapes adapt to mechanical stresses from organ-scale growth. In many plants, epidermal cells form puzzle shapes characterized by intricate lobes and indentations, which reduce mechanical stress during expansion. Yet, the role of organ-scale growth in shaping these cells remains unclear. Here, we examine how growth dynamics influence puzzle cell formation. By integrating computational modeling with confocal microscopy, we show that growth history determines cell shape. Cells that start with uniform (isotropic) growth develop complex puzzle-like shapes, while those that begin with directed (anisotropic) growth stay simple and elongated. If growth later shifts to isotropic, cells gain lobes along their earlier growth axis. This suggests that puzzle cell patterns reflect how growth changed over time. Quantitative analyses further show a strong correlation between increasing cell size and enhanced lobeyness, supporting the idea that puzzle shapes arise as adaptive responses to mechanical constraints imposed by organ-scale growth. Disrupting lobed cell morphology in Arabidopsis, through genetic mutations or pharmacological treatments, either restricts growth or triggers compensatory elongation, supporting the role of puzzle-shaped cells in maintaining tissue integrity. Cross-species comparisons reveal extensive plasticity in puzzle cell shapes, varying notably across organs, growth conditions, and developmental stages. Additionally, a broad phylogenetic survey of vascular plants, including both living and fossil species, confirms puzzle cell formation as a conserved trait shaped by developmental and environmental contexts. These findings support the hypothesis that puzzle cell shapes are an adaptive response to developmental constraints, mitigating mechanical stress during growth.

Keywords: mechanical stress, growth, cell shape, pavement cells, puzzle cells

Introduction

The shapes of plant organs, whether broad or elongated, are often reflected in the shapes of individual cells, suggesting a close relationship between organ growth patterns and cellular morphology [1-3]. Studies using Arabidopsis (*Arabidopsis thaliana*) mutants have demonstrated that alterations in organ shape are accompanied by corresponding changes in cell shape and vice versa, highlighting the interdependence of growth dynamics at multiple scales [4-7]. Additionally, integrating experimental biology with theoretical modeling has advanced our understanding of how genes, mechanics, and growth interact, emphasizing the need to view tissues and organs as integrated systems rather than isolated components [8]. These findings suggest that cell shape emerges from collective tissue dynamics rather than being solely determined by molecular regulation of individual cells [9,10].

Endoreduplication, characterized by successive rounds of DNA replication without cell division, results in significant cell enlargement, increasing the mechanical demands on cell walls to withstand the elevated stress from turgor pressure in larger cells [11,12]. In organs such as stems and hypocotyls, cells typically elongate along the main growth axis. This elongated shape naturally limits the stress, which can be estimated by the Largest Empty Circle (LEC), the largest circular area within a cell without internal anticlinal walls, thus reducing mechanical stress [13-15]. However, more isotropic growth in broad aerial organs like leaves presents a distinct challenge, as cells expanding isotropically risk developing large, mechanically vulnerable areas that could rupture due to internal stress [2,16]. To address this, epidermal cells frequently adopt a puzzle-shaped morphology with interlocking lobes. These lobes effectively reduce the LEC, thus minimizing stress-induced deformation and maintaining tissue integrity [15,17,18]. Finite element modeling and stress analysis on puzzle cell shapes provides a functional explanation for these unusually shaped cells, demonstrating that lobed shapes significantly lower mechanical stress during more isotropic expansion. These results link cell shape formation, driven by endoreduplication-induced enlargement, to mechanical constraints and organ-scale growth dynamics, emphasizing mechanical stress as a critical regulator of epidermal cell morphology [15].

At the cellular level, plant cells are tightly connected by their cell walls, meaning that their growth must be coordinated to maintain tissue integrity. This coordination relies on the interplay between internal turgor pressure and the mechanical properties of the cell wall. Turgor pressure generates tensile in-plane stress across the cell wall, which resists expansion while the wall is remodeled in a controlled fashion. Such remodeling includes the regulated sliding of cellulose fibers at specific attachment points, allowing the cell to grow without compromising its structure [14]. Cortical microtubules guide the localized deposition of cellulose microfibrils, thereby stiffening specific regions of the cell wall and reinforcing cell structure. In puzzle-shaped cells, microtubules accumulate in narrow neck regions between protruding lobes, restricting local expansion and shaping the lobed contour, whereas in elongated cells they align transversely to limit lateral growth [13,19-21]. A spring-based model proposes that mi-

crotubule-guided cellulose deposition creates localized zones of stiffness that regulate cell expansion; small surface indentations attract microtubules and become reinforced, while lobes expand relatively freely, establishing a feedback loop that promotes lobe formation [15]. Computational simulations based on this approach have successfully reproduced a variety of cell shapes, capturing significant variation seen in nature, demonstrating its effectiveness in capturing the dynamics of puzzle cell shape acquisition.

A positive correlation between cell area and lobe number has been observed in Arabidopsis and several other species [15]. However, the universality of this relationship remains uncertain as environmental factors, such as drought, temperature, and light, that influence cell and tissue development may also affect stress-based shape acquisition. In a broader survey of vascular plants, Vőfély, et al. [22] found no correlation between cell area and lobe number, suggesting that highly undulating cell margins, like those in Arabidopsis, are relatively rare. This implies that pavement cell shapes may serve diverse functional roles across taxa, representing species-specific adaptive strategies shaped by ecological and evolutionary pressures.

In our study, we address how organ-scale growth dynamics influence cell morphology. We demonstrate that the formation of puzzle-shaped cells is a dynamic response to growth, serving as a mechanism to mitigate mechanical stress as cells increase in size. This finding suggests that variations in tissue growth not only shape the final morphology of individual cells but also mirror the developmental history of the organ. Time-lapse observations in maize (*Zea mays*) leaves revealed that shifts in growth anisotropy are closely linked to the emergence of complex cell shapes. Computational modeling further indicated that tissue growth dynamics directly influence puzzle cell formation, with the growth history of tissues playing a crucial role in determining final cell morphology. Suppression of lobe formation results in dwarf phenotypes or triggers compensatory alterations in cell shape to sustain organ growth. Furthermore, our results indicate that cell shape acquisition is a highly dynamic and plastic process, with variations that correlate with developmental stage, organ type, and environmental conditions. Whether these factors directly influence cell shape or simply modulate the underlying growth dynamics remains an open question. Collectively, our findings support the hypothesis that the interplay between organ-scale growth dynamics and mechanical constraints drives puzzle cell formation, serving as an adaptive strategy to mitigate mechanical stress and maintain tissue integrity during growth.

Results

Impact of organ growth dynamics on puzzle cell formation

The spring model proposed by Sapala, et al. [15] provides a mechanistic explanation for the formation of shapes that maintain small LECs, ranging from puzzle shaped to elongated cells. This model offers a framework not only for understanding how shape emerges at the cellular level but also provides an unexplored opportunity to study the interaction of mechanical constraints and growth dynamics at the organ scale. To empirically validate this model, we ex-

amined the distribution of cortical microtubule orientation in experimentally observed epidermal pavement cells. By analyzing the cell wall morphology and microtubule patterns (**Figure 1A**) and using these observations to create segmented cell models for simulation, we successfully replicated the microtubule dynamics predicted by the model. Simulated connections corresponding to cortical microtubules and downstream cellulose deposition were more concentrated in the indentations and notably sparse in the lobed regions of the cells (**Figure 1A, B**). These results demonstrate that the Sapala, et al. [15] model can generate realistic puzzle cell shapes with microtubule patterns that match experimental observation.

Growth anisotropy significantly influences epidermal cell shape, generally producing elongated cells under anisotropic conditions and puzzle-shaped cells during isotropic growth [15]. Building upon this finding, we further explored how temporal changes in growth anisotropy affect cell morphology, even when the cumulative growth over a given period is the same. We conducted computational simulations starting from an initial template of isodiametric cell shapes (**Figure 1C**), expanding the cells 16 times vertically and 10 times horizontally. In the first scenario, we applied uniform growth rates across all cells with an anisotropic ratio of 1.6:1, resulting in slightly elongated cells with lobes similar to the isotropic case (**Figure 1D, Suppl. Movie 1**), closely resembling cells observed in some areas of the leaf in Arabidopsis. In a second scenario, we initially imposed isotropic growth followed by a brief period of vertical anisotropic growth (approximately 5/6 isotropic and 1/6 anisotropic), which led to vertically oriented lobes (**Figure 1E, Suppl. Movie 2**). Conversely, reversing this sequence, starting with strong anisotropic growth followed by isotropic growth, resulted in horizontally biased lobes (**Figure 1F, Suppl. Movie 3**). These simulations indicate that differences in the temporal dynamics of growth anisotropy, even under conditions of identical cumulative growth, lead to significant variations in cell shape (**Suppl. Figure 1**). Furthermore, isotropic tissue growth tends to yield more complex, puzzle-like cell morphologies, while anisotropic growth produces simpler, elongated forms. These observations suggest that the epidermal cell shape can provide insights into the growth history of plant organs.

To validate the predictions of the model, we investigated the epidermis of maize, where cells are elongated but exhibit puzzle-like shapes at specific distances from the intercalary meristem. These hybrid shapes are particularly intriguing as they are neither fully elongated nor entirely lobed. Using time-lapse experiments, we obtained sequential replicas of cell patches on juvenile maize leaves, covering different distances from the intercalary meristem. This approach allowed us to reconstruct the morphogenesis of maize pavement cells using two consecutive time points (**Suppl. Figure 2**). Our observations revealed that maize puzzle cells develop through an initial phase of strong longitudinal anisotropic growth, which transitions into a less anisotropic phase where transverse growth stabilizes. This sequential growth promotes the emergence of puzzle-like cell shapes at specific developmental stages (**Figure 1G**). To simulate maize cell development, we initialized the model with a representative geometry of young cells (**Figure 1H**). By adjusting growth rates and anisotropy based on time-lapse

observations, we reproduced the shapes and timing of maize puzzle cells (**Figure 1I, Suppl. Movie 4**). Perturbing the model by reversing the growth sequence, initiating with transverse growth followed by longitudinal growth, produced cell shapes that were substantially different from those observed in maize (**Figure 1J, Suppl. Movie 5, Suppl. Movie 6**). These findings highlight the critical role of growth fields in determining cell shapes and explain the formation of hybrid pavement cell morphologies. By integrating empirical observations with computational modeling, we demonstrate that variations in growth rates over time drive the diversity of cell shapes observed in plant epidermis, revealing a novel dynamic feedback mechanism in which organ-scale growth dynamics significantly influence individual cell morphology.

Effects of disrupted puzzle cell formation on organ growth

As cells increase in area, they maintain low LEC values to minimize mechanical stress [15]. Cells that expand in two directions reduce the LEC by developing lobes, whereas highly elongated, anisotropically growing cells can enlarge while maintaining small LECs and, therefore, are not expected to develop lobes. To determine how growth in two directions correlates with puzzle-like shapes, we introduced the concept of the *minimum axis* (*min-axis*), defined as the shortest dimension of the cell, measured by the width of the smallest rectangle that fully encloses it (**Figure 2A**). This measure better reflects the aspect of cell size relevant to mechanical stress; long, thin cells have low min-axis values, while cells that are large in both length and width exhibit higher min-axis values, which are expected to be positively correlated with lobeyness. Lobeyness is defined as the ratio of a cell perimeter to the perimeter of its convex hull, the inverse measure of convexity (**Figure 2A**) This measure is particularly effective at distinguishing lobey cells from long, thin cells with gentle curves but no pronounced lobes (*e.g.,* boomerang-shaped cells) [15]. By integrating the min-axis and lobeyness metrics, we provide a more robust framework for quantifying and distinguishing cell shapes, enabling better insights into the relationship between cell growth dynamics and mechanical stress. Our analysis of Arabidopsis revealed a stronger correlation between min-axis and lobeyness than between cell area and lobeyness (**Figures 2B-F**), consistent with the idea that combined min-axis and lobeyness better reflect mechanical constraints and stress-mitigation strategies.

To explore how changes in cell shape influence organ shape and growth, we analyzed pavement cell morphology along with leaf and whole-plant phenotypes in mutants with defective puzzle cell formation and in wild-type plants subjected to pharmacological treatments. In mutants where puzzle shapes were absent, we did not observe cell rupture or death, as reported at the shoot apical meristem [15]. This suggests that these cells may either experience lower mechanical stress, possibly due to changes in the arrangement of neighboring cells and tissue structure, or they might activate compensatory mechanisms, such as restricted organ growth, increased cell elongation or altered cell wall properties, in response to the absence of puzzle-like lobes. Compared to the wild-type Arabidopsis (**Figure 3A, Suppl. Figure 3A**), the con-

195 stitutively active Rho-of-Plants 2 (*CA-ROP2*) mutant, which alters actin filament accumula-
196 tion, displayed non-lobed cells [4]. While lobeyness was abolished in *CA-ROP2*, the lack of
197 lobes was partially compensated by elongated shapes (**Figure 3B, Suppl. Figure 3B**). Im-
198 portantly, *CA-ROP2* mutants exhibited relatively mild reductions in overall plant growth,
199 maintaining taller stature due to their more anisotropic growth habit, suggesting that puzzle
200 cell formation inhibition in this line primarily impacts isotropically growing organs. Similar-
201 ly, the *anisotropy1* (*any1*) mutant, which carries a mutation in cellulose synthase A1 (CesA1)
202 affecting crystalline cellulose synthesis [23], also lacked lobes but exhibited sinuous cells as a
203 compensatory feature (**Figure 3C, Suppl. Figure 3C**). We analyzed the *constitutive triple*
204 *response* (*ctr1*) mutant, a negative regulator of ethylene signaling, which displayed reduced
205 cell expansion and lobeyness, with small cells and smaller leaves (**Figure 3D, Suppl. Figure**
206 **3D**). Collectively, these mutants indicate that if cells are unable to form lobes, they develop
207 compensatory mechanisms, such as elongation or a zigzag morphology, to minimize mechan-
208 ical stress. Notably, all mutants with altered lobeyness exhibited lower correlations between
209 min-axis and lobeyness, along with smaller leaves and overall reduced plant growth com-
210 pared to wild type (**Figure 3E-H**). These observations suggest that the inability to produce
211 lobed cells not only hampers epidermal cell expansion but also has a notable impact on over-
212 all plant growth, highlighting the importance of puzzle-shaped cells in facilitating proper leaf
213 development.

214 Another way to compensate for the lack of lobes is maintaining small, isotropic cell shapes
215 through increased division activity. To further explore the connection between cell shape and
216 division activity we studied mutants of LOSS OF GIANT CELLS FROM ORGANS (LGO),
217 a regulator of endoreduplication [24]. The *lgo-2* mutant, which exhibits reduced endoreduplica-
218 tion in comparison to Col-0, shows increased division activity and small, less-lobed cells
219 (**Suppl. Figure 4A, B**). Conversely, the LGO overexpression line displayed giant cells with
220 highly lobed outlines (**Suppl. Figure 4C**). These results indicate that increased division activ-
221 ity leads to smaller, less-lobed cells, as cells with low LEC values are less likely to develop
222 lobes (**Suppl. Figure 4D**).

223 To complement genetic studies, we used pharmacological treatments to transiently disrupt
224 lobe formation in wild-type Arabidopsis. Treatments with oryzalin, a microtubule depolymer-
225 izer, and latrunculin B, an actin polymerization inhibitor, were performed on cotyledons to
226 examine the effects of inhibiting lobeyness. By employing dose- and time-dependent treat-
227 ments, we precisely regulated the inhibitory effects. Compared to control samples (**Figure**
228 **3I**), low doses of oryzalin led to wider neck regions and larger LECs (**Figure 3J, K**). Higher
229 doses further reduced lobeyness, and at very high concentrations, puzzle cell formation was
230 completely abolished, resulting in nearly isodiametric cell shapes (**Figure 3L, M**). Latruncu-
231 lin B treatments reduced lobeyness by reducing indentation depth, but even at high doses,
232 lobe formation was not entirely eliminated (**Figure 3N-Q**), in contrast to oryzalin treatments.
233 These treatments produced phenotypic responses similar to those observed in mutants, in-

cluding reduced cotyledon sizes and overall inhibited plant growth. Altogether, our results suggest that proper organ growth depends on mechanical constraints that regulate cell shape, while disruptions in cell shape led to defects in organ growth. The absence of lobes disrupts the balance between growth promotion and mechanical resistance, resulting in smaller cells and tissues, ultimately reducing overall plant size.

Pavement cell shape reflects the developmental and environmental context of the plant

We have shown that epidermal pavement cell shape can depend on the growth dynamics of the organ in which they develop. This raises the question of how many plant species can form puzzle cells, even if they do not display this feature in leaves grown in a particular environment. To address this question, we examined epidermal pavement cells across various developmental stages, organs, and environmental contexts. Pavement cells exhibit diverse shapes that vary not only across species but also among different organs within the same plant. Their morphology is influenced by developmental stage, environmental conditions, and tissue-specific cues, all of which alter growth dynamics and ultimately determine the extent of lobe formation [25-27]. We first examined how developmental stage affects cell shape by comparing pavement cells in juvenile and mature leaves of various species. In quaking aspen (*Populus tremuloides*), juvenile leaves were less lobed than mature leaves, as indicated by a min-axis-lobeyness correlation of 0.46 in juvenile leaves and 0.67 in mature leaves (**Figure 4A, D, G**). Similar trends were observed in lilac (*Syringa vulgaris,* **Suppl. Figure 5A, B**) and camphor tree (*Camphora officinarum*, **Suppl. Figure 5C, D**). Notably, in lilac, cells previously reported as non-lobed [22] appeared lobed in our dataset, likely reflecting differences in developmental stage or environmental conditions. The timing of puzzle-shape formation varied across species, with some plants delaying this process until later developmental stages. We frequently observed a coexistence of lobed and non-lobed cells within the same plant, or even within the same organ. For example, in elderberry (*Sambucus nigra*) leaves (**Suppl. Figure 6A**) and in the bracts of linden (*Tilia cordata*; **Suppl. Figure 6B**), cells situated above vascular tissues were elongated, while those above the mesophyll were lobed. Similarly, in early developing Arabidopsis leaves, the proliferative base contains isodiameteric cells, with puzzle-shaped cells emerging distally in the more differentiated regions where division has ceased [2,28].

We also observed differences in pavement cell morphology between the abaxial (lower) and adaxial (upper) surfaces of the same leaf. For instance, in species such as love-lies-bleeding (*Amaranthus caudatus*; **Suppl. Figure 7A-C**), Peruvian-lily (*Alstroemeria aurea*; **Suppl. Figure 7D-F**), fuchsia (*Fuchsia magellanica*; **Suppl. Figure 7G-I**), peppermint (*Mentha x piperita*; **Suppl. Figure 7J-L**), and cigar flower (*Cuphea ignea*; **Suppl. Figure 7M-O**), the abaxial surface exhibited more pronounced lobing than the adaxial surface, which is directly exposed to sunlight [29]. These findings highlight the influence of developmental context and positional cues on cell morphology.

Environmental factors also significantly influence pavement cell shape. In camphor tree leaves, typically characterized by non-lobed cells in leaf epidermis [30], cells developed puzzle shapes when grown in greenhouse conditions, with the min-axis-lobeyness correlation of 0.59, whereas this morphology was not observed when plants were cultivated outdoors with a correlation of 0.3 (**Figures 4B, E, H**). Interestingly, the camphor tree appears somewhat unusual because, although outdoor-grown cells were larger, they remained non-lobed, while smaller indoor-grown cells adopted a puzzle-like morphology. Given that both indoor and outdoor cells are very small, the absence of lobes outdoors does not seem mechanically driven; rather, the formation of lobes indoors may reflect other environmental signals beyond mechanical stress, such as variations in light intensity or spectral quality. Thus, these observations suggest that lobe formation may not be solely a direct response to mechanical stress but can integrate diverse environmental signals. Overall, our results are consistent with the idea, also proposed by Vőfély, et al. [22], that making puzzle shapes is an actionable mechanism to adapt to the environment, and not only a passive consequence of the environment such as sun exposure or humidity. Similarly, these observations align with paleoecological studies that use cell sinuosity to distinguish sun and shade leaves and to infer environmental dynamics [31,32].

To determine whether lobed cells form in other organs when absent from leaves, we examined pavement cells in various organs, including petals, sepals, and fruits. In certain species, such as linden (*Tilia cordata*; **Figure 4C**) and crownvetch (*Securigera varia*; **Suppl. Figure 8A**), the epidermal pavement cells on the adaxial side of mature leaves were non-lobed. This observation prompted us to investigate whether the mechanism for lobe formation is present but not expressed in leaves. Our findings revealed that, despite the absence of lobes in leaves, lobed cells did appear in other organs, for example, in the bracts of linden (**Figure 4F**) or the petals of crownvetch (**Suppl. Figure 8B**). Interestingly, in linden, elongated bracts exhibited a min-axis/lobeyness correlation of 0.85, whereas rounder leaves showed a correlation of only 0.16 (**Figure 4I**). This phenomenon was widespread across species (**Suppl. Figure 8C-L**), including petals in cemetery iris (*Iris albicans*) and spring crocus (*Crocus vernus*), as well as sepals in St John's wort (*Hypericum perforatum*), common gorse (*Ulex europaeus*) and blackthorn (*Prunus spinosa*). In these species, lobed cells were absent in leaves but present in other organs. These results suggest that while the program for lobe formation exists in these plants, its expression is organ-specific, offering new opportunities to study the regulation of complex cell shape acquisition beyond leaves.

Prevalence and function of puzzle shapes in limiting mechanical stress

To assess the universality of lobe formation in response to increasing cell size, we conducted a large-scale analysis of the correlation between the min-axis and lobeyness across vascular plant species (**Figure 5A**). We analyzed cell shapes in 327 species and 663 species-organ combinations, totaling 72,026 cells (**Suppl. Table 1**). In our analysis, we collected samples from 45 species in various plant organs and incorporated data from previously published

analysis of leaf epidermal pavement cells in 19 species Sapala, et al. [15], 250 species from Vőfély, et al. [22], and data from 13 early Miocene species [33]. In 235 of 327 species (72%), we observed a moderate or higher positive correlation (≥ 0.3) between min-axis and lobeyness, with particularly high correlations found in tobacco (*Nicotiana tabacum*, Corr = 0.96), cigar plant (*Cuphea ignea*, Corr = 0.90), morning glory (*Ipomoea tricolor*, Corr = 0.91), black nightshade (*Solanum nigrum*, Corr = 0.90), Java fern (*Microsorum pteropus*, Corr = 0.85), and Peruvian lily (*Alstroemeria aurea*, Corr = 0.89) (**Suppl. Figure 9A–F**, **Suppl. Figure 10A**).

Because plant organs typically contain a mixture of lobed and non-lobed cells, the average cell shape may not capture the full capacity of a species to produce puzzle-shaped cells. To address this, we determined the ability of each species to develop lobed cells by using the 95th percentile of cell lobeyness, which effectively captures the upper range of lobing across different organs and developmental contexts (**Figure 5B, C**). This metric revealed that most species possess the capacity to generate highly lobed cells, even if the average cell shape does not exhibit significant lobeyness as previously reported by Vőfély, et al. [22]. Overall, these findings, together with the species-wide correlations and organ-specific analyses, demonstrate that cell shape is highly plastic and influenced by developmental, environmental, and organ-specific factors, with the ability to form lobed cells representing a widespread adaptive strategy for managing mechanical stress during growth.

However, some species displayed weak or even negative correlations between the min-axis and lobeyness (**Figure 5A**), which seems contradictory to the notion that lobes form in response to a developmental constraint based on stress. Upon further examination of these cases, we identified several reasons for the lack of a strong correlation in certain samples. In cardboard palm (*Zamia furfuracea*), the highly anisotropic growth led to elongated cells without an increase in the min-axis, thus not favoring lobe formation (**Suppl. Figure 9H, Suppl. Figure 10B**). Conversely, species like yellow guava (*Psidium guajava*) and pinwheel flower (*Tabernaemontana divaricata*) maintained a small uniform cell size, suggesting frequent divisions to maintain size, even though the leaves can become quite large (**Suppl. Figure 9G, J, Suppl. Figure 10C, D**). Weak correlations were also seen in some species with highly lobey cells, such as hare's foot fern (*Davallia solida*; **Suppl. Figure 9I, Suppl. Figure 10E**). The min-axis does not capture this case well, as substantial variability comes from branching rather than an increase in lobes, as the cells are all highly lobey. Here, it would be better to sample a patch of the leaf where the cells have a gradient from smaller dividing cells to mature expanded ones. In species without lobes, like agapanthus (*Agapanthus praecox*), cell staggering had a greater impact on thinner, less elongated cells (**Suppl. Figure 9L, Suppl. Figure 10F**), whereas in Virginia spiderwort (*Tradescantia virginiana*), the irregular shapes of smaller stomatal lineage cells contributed to higher lobeyness scores (**Suppl. Figure 9K, Suppl. Figure 10G**). Overall, our analysis shows that species that made lobed cells

had significant positive correlation between lobeyness and min-axis, and that species where this correlation was absent largely fall into a small number of well-defined classes.

Our hypothesis is that the puzzle cell shape helps to reduce stress as the cell gets larger by controlling the size of the LEC. Consequently, compared to small cells, large cells are expected to exhibit a smaller increase in LEC for the same increase in area. To test this prediction, we plotted cell area vs LEC and used a quadratic fit line passing through the origin (**Suppl. Figure 11A**). If our hypothesis holds, the curve should bend to the right ($\alpha < 0$), indicating that the LEC area increases more slowly than cell area. This pattern is exactly what we observed (**Suppl. Figure 11B, C**). Moreover, since uncontrolled expansion in all directions would proportionally increase LEC, cells must preferentially become either elongated or lobed. Using the min-axis as a proxy for directional growth, we found that LEC area increases more slowly than the min-axis (**Suppl. Figure 11D, E**), a relationship that persisted across multiple clades and species (**Suppl. Figure 11F-K**). Overall, 87% of species (286 of 386) exhibited negative α values (**Suppl. Figure 12**). An exact sign-test confirms that this pattern is highly unlikely to occur by chance ($p < 0.05$), indicating that LEC area increases more slowly than the min-axis. This finding supports our hypothesis that, rather than expanding proportionally, cells tend to become more lobed (or snake-like) to limit the wall free span and reduce tensile stress.

Discussion

Since the epidermis plays a pivotal role in shaping plant organ architecture [34,35], it is essential that its cells possess robust mechanisms to sense, adapt to, and mitigate mechanical stress. Here we show that puzzle cell shapes emerge as a result of the tight interaction between mechanical constraints and growth at the organ scale; however, the great diversity of the cell shapes observed in epidermis raises the question of how those various shapes are acquired. Our analysis of epidermal pavement cells in maize leaves and computational modeling underscore the critical role of specific growth trajectories in shaping puzzle cells, suggesting that the morphology of these cells may offer insights into the growth history and environmental adaptations of both living and extinct plant species [36]. The observed variation in the presence or absence of puzzle cells across different contexts likely reflects differences in growth and proliferation dynamics rather than fundamental differences in the mechanism of puzzle cell patterning. Consequently, a gene influencing growth rate, timing, directionality, or cell division could affect the manifestation of the puzzle cell phenotype, regardless of its direct involvement in the lobe patterning process itself. Similarly, genetic modifications that affect growth can alter cell shape; for example, *ftsh4* mutants exhibit increased organ shape variability and enhanced lobing due to altered ROS levels, while *LONGIFOLIA1* overexpression leads to elongated cells and organs with reduced lobing [15,37]. Likewise, genes that promote cell proliferation may lead to the formation of smaller, less lobed cells, as observed in the *lgo-2* mutant (**Suppl. Figure 4B, D**). Conversely, genes that inhibit cell division and promote cell expansion, such as those involved in endoreduplication, may result in larger, more lobed

388 cells, as seen in the *LGO OX* line (**Suppl. Figure 4C, D**). Interestingly, recent work has
389 found a relationship between mechanical stress levels and lobe width in puzzle cells, with
390 increased stress leading to wider lobes [38], suggesting that mechanical forces can directly in-
391 fluence cell shape. This intertwining of growth regulation and cell proliferation with the de-
392 velopment of puzzle cell shapes highlights the importance of distinguishing between genes
393 specifically affecting the mechanisms of puzzle cell formation from those controlling growth.

394 Studies on mutants and pharmacological treatments indicate that puzzle cell formation is a
395 strategic response to mechanical stresses, driven by growth-restriction mechanisms that may
396 be common among higher plants. Although we cannot definitively claim broad conservation
397 based solely on these experiments, our findings are consistent with the idea that the underly-
398 ing mechanism involves microtubule-guided cellulose deposition, which restricts growth in
399 localized regions of the cell wall. Pharmacological treatments using oryzalin and latrunculin
400 B further support this model. Oryzalin, which depolymerizes microtubules, disrupts localized
401 cell wall reinforcement in the neck regions of developing puzzle cells, while latrunculin B, by
402 inhibiting actin polymerization, impairs the targeted delivery of key cell wall components
403 [4,19,39]. Together, these results confirm the Sapala, et al. [15] model prediction that puzzle cell
404 formation relies on regulated growth restriction mediated by cellulose microfibrils and asso-
405 ciated mechanical 'springs', rather than by unrestrained cellular outgrowths. Arabidopsis mu-
406 tants unable to form puzzle cells exhibit stunted growth, underscoring the importance of these
407 structures for normal development. While some plants developed snaky cells as a compensa-
408 tory response to the absence of puzzle cells, this alternative morphology does not fully restore
409 normal cell formation and is rarely observed in both extant and fossil records, suggesting that
410 it may be evolutionarily disfavored compared to the more common and adaptable puzzle cell
411 morphology. Collectively, these observations support the view that puzzle cell formation is a
412 strategic response to mitigate the high mechanical stresses that would be created in large iso-
413 diametric cells, and that it is mediated by growth restriction, a process that is likely broadly
414 conserved in higher plants.

415 Despite the apparent complexity of factors influencing puzzle cell formation, their wide-
416 spread emergence reflects a response to a physical constraint shared by all plants. Puzzle cell
417 formation is essential in organs with large, isotropically growing cells to prevent the for-
418 mation of extensive, unreinforced areas that would bulge out under high mechanical stress.
419 However, various factors can prevent the formation of puzzle-shaped cells even in species
420 capable of producing them, since plants can employ alternative strategies to cope with me-
421 chanical stress. One option is that the small, isotropic cell shapes observed in species such as
422 yellow guava (*Psidium guajava*) may indicate that cells continue to divide, preventing them
423 from enlarging excessively and thus reducing the need for puzzle cell formation. Alternative-
424 ly, many plants transition from actively dividing, meristematic cells to larger, endoreduplicat-
425 ed cells (**Suppl. Figure 4**), a process common in the epidermis of leaves, roots, and sepals of
426 Arabidopsis, that often promotes puzzle cell formation as cells expand. In roots and hypocot-

yls, growth is highly anisotropic resulting in large but elongated cells; in these cases, the elongated shape minimizes open areas, rendering puzzle cell formation unnecessary. However, in organs where growth is less anisotropic, such as leaves and cotyledons, larger cells adopt the puzzle shape to mitigate bulging and mechanical stress. Under isotropic growth conditions, the absence of puzzle cells would lead to the development of large, unreinforced regions in the periclinal cell wall, exposing cells to considerable turgor-induced stress. Another strategy to manage stress in large, isodiametric cells is to develop thicker cell walls; however, this approach is less common, likely because it requires substantially more resources than forming a complex cell shape with lobes and indentations [40]. Our large-scale analysis of pavement cells across vascular plants, including plant organs beyond leaves such as sepals, bracts, and even fossil species [33], showed that most species contain cells that exhibit significant puzzle cell shapes (**Figure 5**), whereas species lacking puzzle cells tend to have elongated cells or cells with small sizes. Interestingly, we found that while some species may not exhibit puzzle cells in their leaves, they can still form them in other organs, such as sepals or bracts, and that the appearance of puzzle cells is influenced by developmental stage and environmental conditions. Overall, our integrated analysis reveals that puzzle cell formation is a dynamic, evolutionarily conserved strategy that enables plants to optimize cell and tissue integrity in response to mechanical constraints, thereby ensuring robust organ development across diverse environmental contexts.

Author contribution

Conceptualization: RSS, MM. **Methodology:** NT, RSS, MM. **Investigation:** NT, BL, AP, FC, LH, AM, TR, DK, AR, RSS, MM. **Formal analysis:** NT, FC, DK, AHKR, AR, RSS, MM. **Data curation:** NT, RSS, MM. **Writing – original draft:** MM. **Writing – review & editing:** NT, BL, TR, DK, AHKR, AR, RSS, MM**. Funding acquisition:** NT, LH, AHKR, DK, AR, RSS, MM. **Supervision**: AHKR, RSS, MM.

Acknowledgements

We are grateful to Olivier Hamant, Arezki Boudaoud and Alice Malivert for valuable comments on the manuscript. We thank John Innes Foundation (NT), the University of Lausanne (NT, AP, LH, AM, MM), EMBO Postdoctoral Fellowship (LH), NSF IOS 1553030 (AHKR), the National Science Centre, Poland (SHENG1 grant 2018/30/Q/NZ3/00189) (DK), ERA-CAPS (DK, RSS, MM), the Sciences and Engineering Research Council of Canada Discovery Grant 2021-02795 (AR), and the Biotechnological and Biological Sciences Research Council (BBSRC) Institute Strategic Programme Grant (BB/X01102X/1) to the John Innes Centre (RSS). We acknowledge Dr Izabela Potocka from the Scanning Electron Microscopy Laboratory of Institute of Biology, Biotechnology and Environmental Protection, University of Silesia for help in SEM of replicas. We thank Dr Azahara Martin for providing us with access to the phase-contrast microscope. We would like to thank Prof Geoffrey Wasteneys for providing *any1* seeds, and the Nottingham Arabidopsis Stock Center for distributing other

seeds. The confocal microscopy was performed at the Cellular Imaging Facility (CIF), University of Lausanne.

References

1 Hülskamp, M., Folkers, U. & Grini, P. E. Cell morphogenesis in Arabidopsis. *BioEssays* **20**, 20-29 (1998).

2 Kierzkowski, D. & Routier-Kierzkowska, A. L. Cellular basis of growth in plants: geometry matters. *Curr Opin Plant Biol* **47**, 56-63 (2019). https://doi.org/10.1016/j.pbi.2018.09.008

3 Dong, Y. *et al.* SHOOTMERISTEMLESS autoactivation: A prerequisite for fruit metamorphosis. *bioRxiv*, 2024.2002. 2023.581830 (2024).

4 Qiu, J. L., Jilk, R., Marks, M. D. & Szymanski, D. B. The Arabidopsis SPIKE1 gene is required for normal cell shape control and tissue development. *Plant Cell* **14**, 101-118 (2002). https://doi.org/10.1105/tpc.010346

5 Tasker-Brown, W. *et al.* An incoherent feed-forward loop involving bHLH transcription factors, Auxin and CYCLIN-Ds regulates style radial symmetry establishment in Arabidopsis. *The Plant Journal* **119**, 2885-2903 (2024).

6 Hake, S. *et al.* The role of knox genes in plant development. *Annu. Rev. Cell Dev. Biol.* **20**, 125-151 (2004).

7 Vlad, D. *et al.* Leaf shape evolution through duplication, regulatory diversification, and loss of a homeobox gene. *Science* **343**, 780-783 (2014).

8 Marconi, M. & Wabnik, K. Shaping the organ: a biologist guide to quantitative models of plant morphogenesis. *Frontiers in plant science* **12**, 746183 (2021).

9 Pérez-Henríquez, P. *et al.* Hierarchical global and local auxin signals coordinate cellular interdigitation in Arabidopsis. *BioRxiv* (2024).

10 Pérez-Henríquez, P. *et al.* PIN2-mediated self-organizing transient auxin flow contributes to auxin maxima at the tip of Arabidopsis cotyledons. *Nature Communications* **16**, 1380 (2025).

11 Roeder, A. H. *et al.* Variability in the control of cell division underlies sepal epidermal patterning in Arabidopsis thaliana. *PLoS biology* **8**, e1000367 (2010).

12 Edgar, B. A., Zielke, N. & Gutierrez, C. Endocycles: a recurrent evolutionary innovation for post-mitotic cell growth. *Nature reviews Molecular cell biology* **15**, 197-210 (2014).

13 Baskin, T. I. Anisotropic expansion of the plant cell wall. *Annu Rev Cell Dev Biol* **21**, 203-222 (2005). https://doi.org/10.1146/annurev.cellbio.20.082503.103053

14 Cosgrove, D. J. Building an extensible cell wall. *Plant Physiology* **189**, 1246-1277 (2022).

15 Sapala, A. *et al.* Why plants make puzzle cells, and how their shape emerges. *Elife* **7** (2018). https://doi.org/10.7554/eLife.32794

16 Hamant, O. & Traas, J. The mechanics behind plant development. *New Phytologist* **185**, 369-385 (2010).

17 Majda, M. *et al.* Mechanochemical Polarization of Contiguous Cell Walls Shapes Plant Pavement Cells. *Dev Cell* **43**, 290-304 e294 (2017). https://doi.org/10.1016/j.devcel.2017.10.017

18 Bidhendi, A. J. & Geitmann, A. Methods to quantify primary plant cell wall mechanics. *Journal of Experimental Botany* **70**, 3615-3648 (2019). https://doi.org/10.1093/jxb/erz281

19 Panteris, E. & Galatis, B. The morphogenesis of lobed plant cells in the mesophyll and epidermis: organization and distinct roles of cortical microtubules and actin filaments. *New Phytol* **167**, 721-732 (2005). https://doi.org/10.1111/j.1469-8137.2005.01464.x

20 Sampathkumar, A. *et al.* Subcellular and supracellular mechanical stress prescribes cytoskeleton behavior in Arabidopsis cotyledon pavement cells. *elife* **3**, e01967 (2014).

21 Paredez, A. R., Somerville, C. R. & Ehrhardt, D. W. Visualization of Cellulose Synthase Demonstrates Functional Association with Microtubules. *Science* **312**, 1491-1495 (2006). https://doi.org/doi:10.1126/science.1126551

22 Vőfély, R. V., Gallagher, J., Pisano, G. D., Bartlett, M. & Braybrook, S. A. Of puzzles and pavements: a quantitative exploration of leaf epidermal cell shape. *New Phytologist* **221**, 540-552 (2019). https://doi.org/https://doi.org/10.1111/nph.15461

23 Fujita, M. *et al.* The anisotropy1 D604N mutation in the Arabidopsis cellulose synthase1 catalytic domain reduces cell wall crystallinity and the velocity of cellulose synthase complexes. *Plant Physiology* **162**, 74-85 (2013).

24 Schwarz, E. M. & Roeder, A. H. Transcriptomic effects of the cell cycle regulator LGO in Arabidopsis sepals. *Frontiers in Plant Science* **7**, 1744 (2016).

25 Ikematsu, S. *et al.* Rewiring of hormones and light response pathways underlies the inhibition of stomatal development in an amphibious plant Rorippa aquatica underwater. *Current Biology* **33**, 543-556.e544 (2023). https://doi.org/https://doi.org/10.1016/j.cub.2022.12.064

26 Majda, M. *et al.* Elongation of wood fibers combines features of diffuse and tip growth. *New Phytol* (2021). https://doi.org/10.1111/nph.17468

27 Zuch, D. T. *et al.* Cell biology of the leaf epidermis: Fate specification, morphogenesis, and coordination. *The Plant Cell* **34**, 209-227 (2022).

28 Fox, S. *et al.* Spatiotemporal coordination of cell division and growth during organ morphogenesis. *PLOS Biology* **16**, e2005952 (2018). https://doi.org/10.1371/journal.pbio.2005952

29 Watson, R. W. The effect of cuticular hardening on the form of epidermal cells. *New Phytologist* **41**, 223-229 (1942). https://doi.org/10.1111/j.1469-8137.1942.tb07075.x

30 Zhao, X. *et al.* Developmental mechanism and distribution pattern of stomatal clusters in Cinnamomum camphora. *Russian Journal of Plant Physiology* **53**, 310-315 (2006).

31 Bush, R. T. *et al.* Cell anatomy and leaf δ13C as proxies for shading and canopy structure in a Miocene forest from Ethiopia. *Palaeogeography, Palaeoclimatology, Palaeoecology* **485**, 593-604 (2017). https://doi.org/https://doi.org/10.1016/j.palaeo.2017.07.015

32 Kürschner, W. M. The anatomical diversity of recent and fossil leaves of the durmast oak (Quercus petraea Lieblein/Q. pseudocastanea Goeppert) — implications for their use as biosensors of palaeoatmospheric CO2 levels. *Review of Palaeobotany and Palynology* **96**, 1-30 (1997). https://doi.org/https://doi.org/10.1016/S0034-6667(96)00051-6

33 Reichgelt, T. *et al.* Elevated CO2, increased leaf-level productivity, and water-use efficiency during the early Miocene. *Clim. Past* **16**, 1509-1521 (2020). https://doi.org/10.5194/cp-16-1509-2020

34 Kutschera, U. & Niklas, K. J. The epidermal-growth-control theory of stem elongation: an old and a new perspective. *J Plant Physiol* **164**, 1395-1409 (2007). https://doi.org/10.1016/j.jplph.2007.08.002

35 Beauzamy, L., Derr, J. & Boudaoud, A. Quantifying hydrostatic pressure in plant cells by using indentation with an atomic force microscope. *Biophys J* **108**, 2448-2456 (2015). https://doi.org/10.1016/j.bpj.2015.03.035

36 Couturier, E., Courrech du Pont, S. & Douady, S. A global regulation inducing the shape of growing folded leaves. *PloS one* **4**, e7968 (2009).

37 Wang, R. *et al.* HSP90 regulates temperature-dependent seedling growth in Arabidopsis by stabilizing the auxin co-receptor F-box protein TIR1. *Nature Communications* **7**, 10269 (2016). https://doi.org/10.1038/ncomms10269

38 Malivert, A. *et al.* FERONIA and microtubules independently contribute to mechanical integrity in the Arabidopsis shoot. *PLoS biology* **19**, e3001454 (2021).

39 Bidhendi, A. J., Altartouri, B., Gosselin, F. P. & Geitmann, A. Mechanical stress initiates and sustains the morphogenesis of wavy leaf epidermal cells. *Cell Reports* **28**, 1237-1250. e1236 (2019).

40 Majda, M., Sapala, A., Routier-Kierzkowska, A. L. & Smith, R. S. Cellular Force Microscopy to Measure Mechanical Forces in Plant Cells. *Methods Mol Biol* **1992**, 215-230 (2019). https://doi.org/10.1007/978-1-4939-9469-4_14

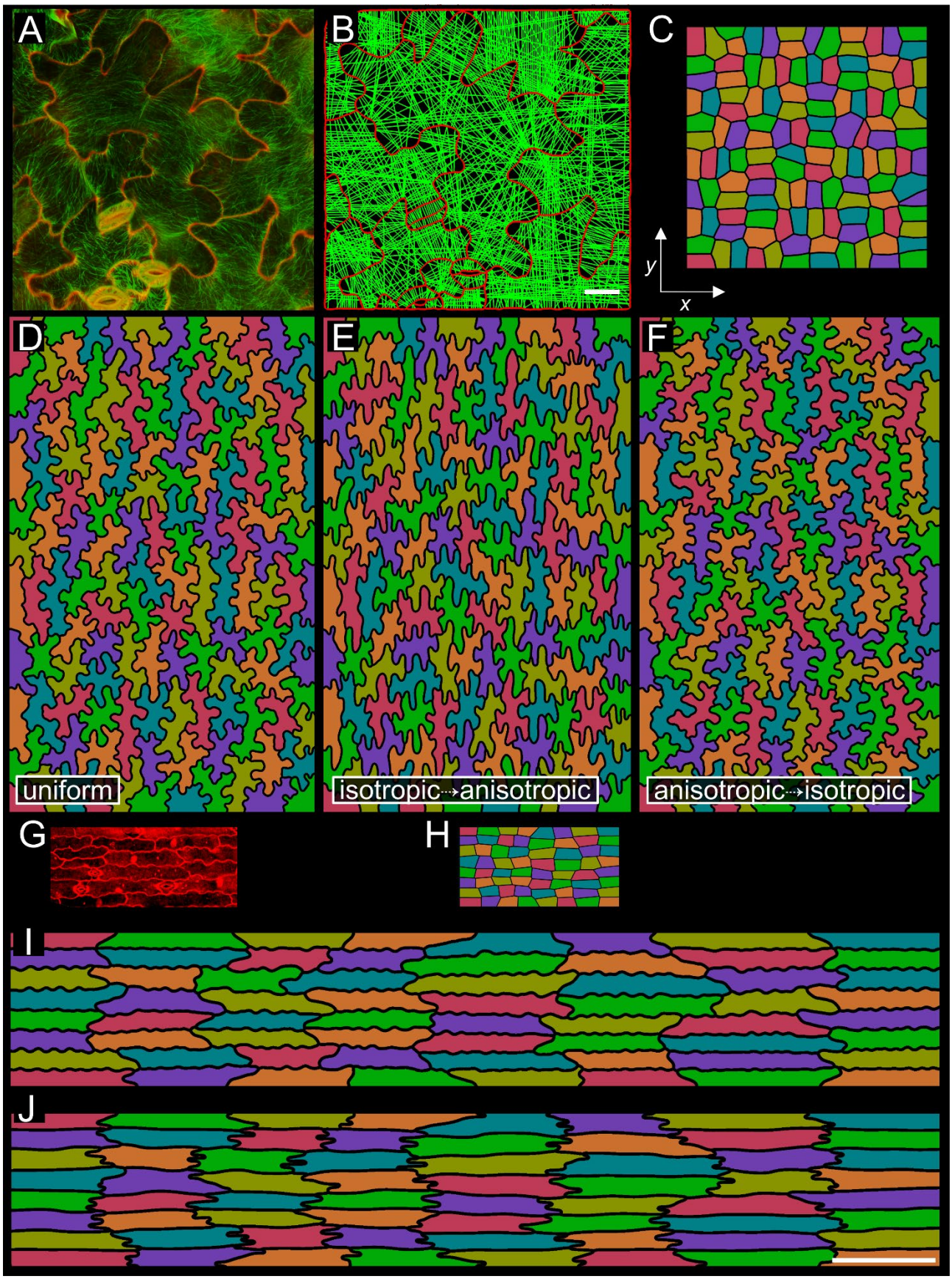

Figure 1. Growth distribution over time influences the shapes of pavement cells. (**A**) Confocal image representing epidermal pavement cells from a fully developed 3-week-old leaf of *Arabidopsis thaliana*. The cell wall was visualized using propidium iodide staining (red), and the microtubules were visualized using fluorescent TUA6-CFP (green). (**B**) A visualization of the placement of connections across the cells for the cell shapes in A in the computational model. (**C-F**)

Model simulation of puzzle cell formation across various growth fields. (**C**) The initial template. (**D-F**) Cell shapes evolved over 300 growth iterations into the same final template size, which is 16 times larger in the y direction and 10 times larger in the x direction than the initial template. (**D**) Uniform weakly anisotropic growth with puzzle-shaped cells. Growth rates in the x and y directions are different but constant over time. (**E**) Initially isotropic growth followed by a short period of anisotropic growth in the y direction only (5/6 vs 1/6 of the simulation time) resulting in puzzle-shaped cells whose lobes are largely oriented vertically. (**F**) The same simulation with the growth reversed, a short burst of anisotropic growth followed by more isotropic growth, resulting in puzzle-shaped cells with a subtle bias in the horizontal orientation. (**G**) Cell shape in maize (*Zea mays*). (**H**) Initial starting template of idealized maize cells. (**I** Cell shapes that emerge when growth in the model initially follows anisotropic growth rates observed experimentally, then switches to more isotropic growth rates. (**J**) The effect on cell shape when the template is first grown in the y direction, then the x direction to reach the same final template size and shape as **I**. Scale bars: (**A**-**B**) 20 μm, (**H-J**) 200 μm.

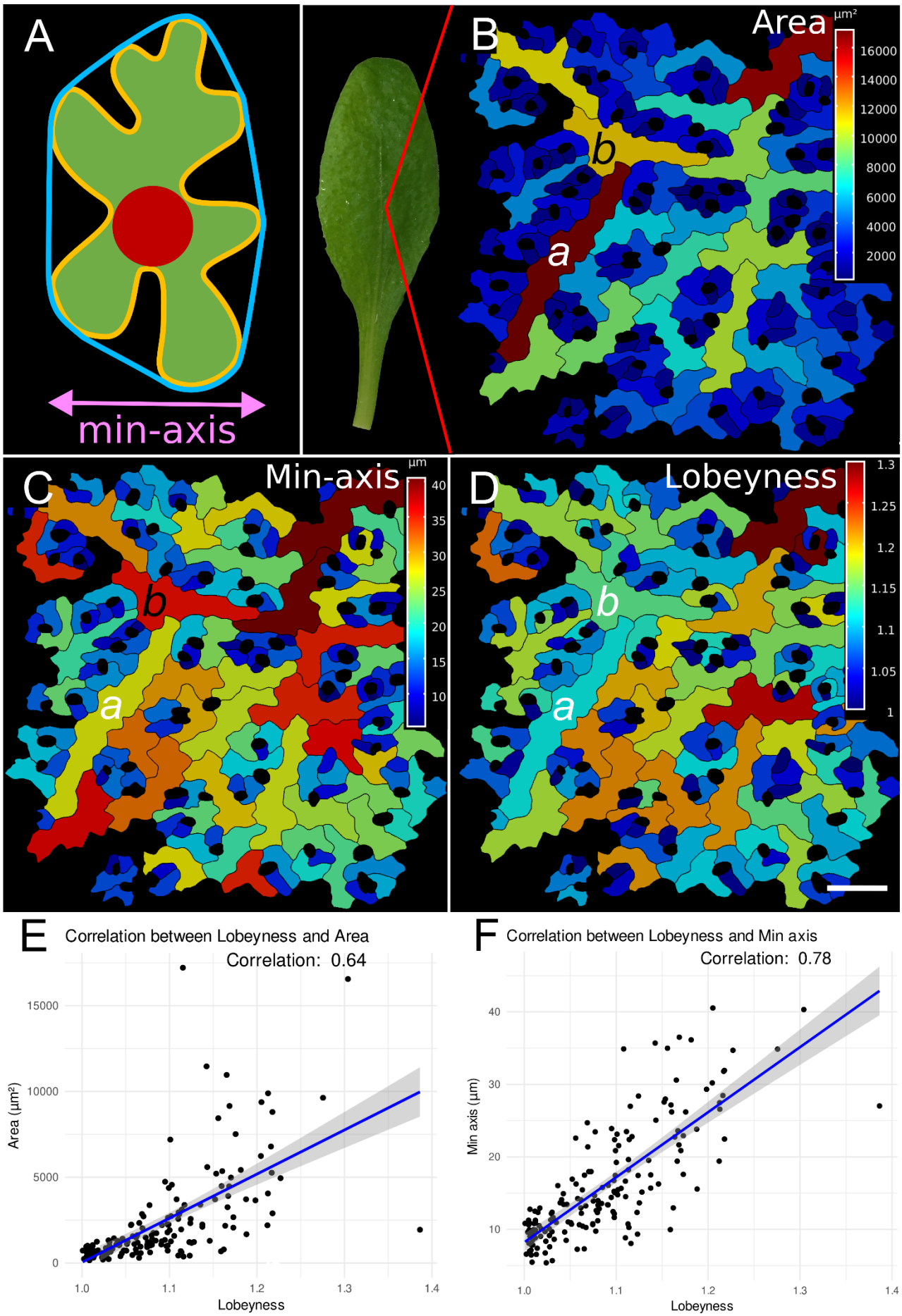
A
min-axis
B
Area
µm²
16000
14000
12000
10000
8000
6000
4000
2000
b
a
C
Min-axis
µm
40
35
30
25
20
15
10
b
a
D
Lobeyness
1.3
1.25
1.2
1.15
1.1
1.05
1
b
a
E
Correlation between Lobeyness and Area
Correlation: 0.64
Area (µm²)
15000
10000
5000
0
1.0
1.1
1.2
1.3
1.4
Lobeyness
F
Correlation between Lobeyness and Min axis
Correlation: 0.78
Min axis (µm)
40
30
20
10
1.0
1.1
1.2
1.3
1.4
Lobeyness

Figure 2. Lobeyness appears widely as a response to increasing cell size. (**A**) The visual depiction of the pavement cell descriptors: area is shown in green, lobeyness is defined as the cell perimeter (yellow) divided by the perimeter of the convex hull (blue), the min-axis (purple) is defined as the smallest width that would fit the cell, and the large open area (LEC) representing the magnitude of mechanical stress (red). (**B-D**) Epidermal pavement cells of a fully developed 3-week-old leaf of *Arabidopsis thaliana* wild type leaf. The cell wall was stained with propidium iodide, imaged with confocal, and then segmented with MorphoGraphX. Epidermal cell templates representing cells colored by area (**B**), min-axis (**C**), and lobeyness (**D**). (**E-F**) Graphs presenting the correlation between area and lobeyness (Corr = 0.64) (**E**) and between min-axis and lobeyness (**F**) for the same sample as in **B-D**. Scale bars: 100 µm (**B-D**).

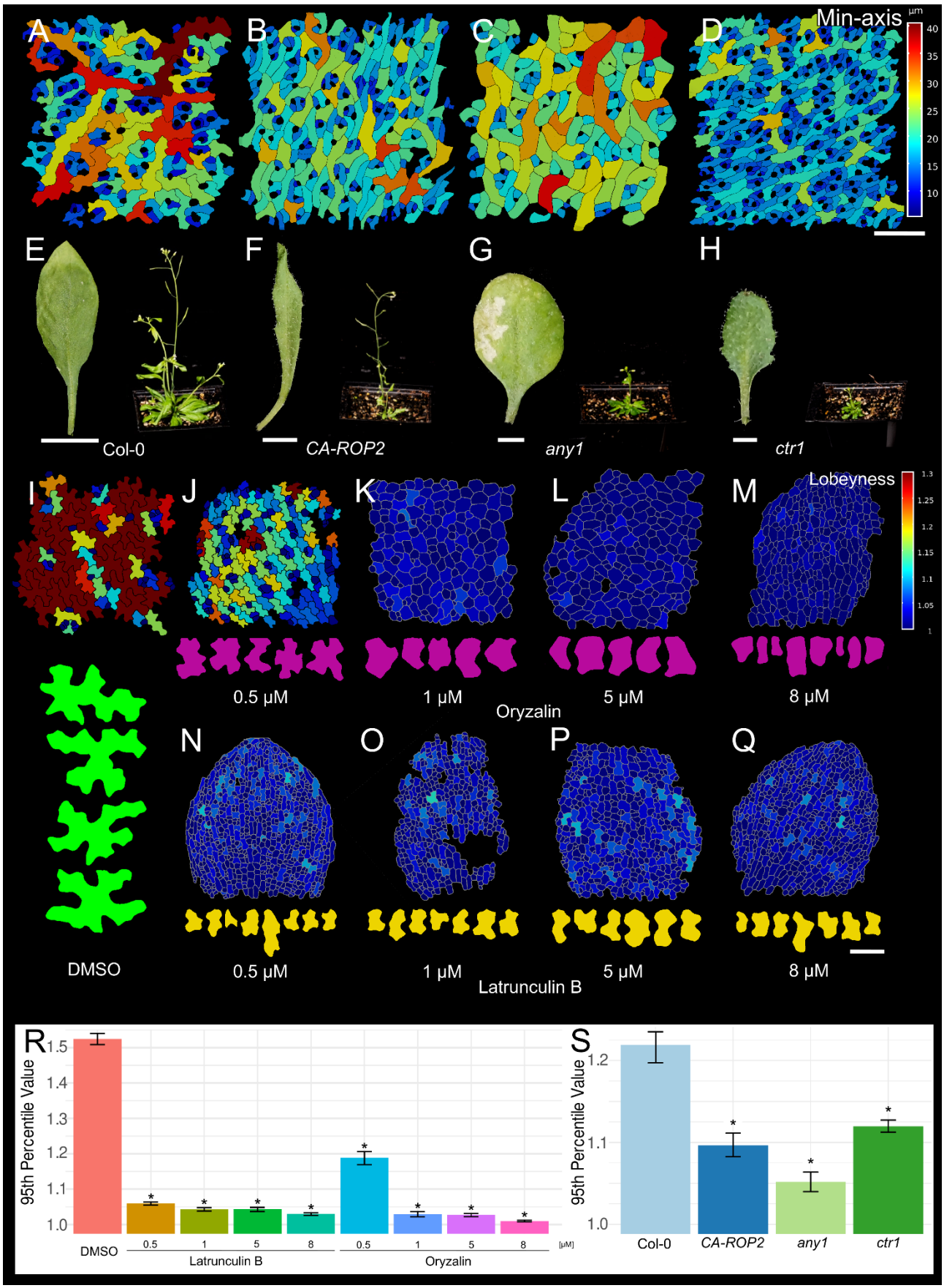

Figure 3: The lack of lobes is associated with growth defects. (**A-H**) The shape of epidermal pavement cells (**A-D**) and overall growth phenotypes (**E-H**) in 3-week-old *Arabidopsis thaliana* wild type (Col-0) and mutants. (**A**, **E**) Puzzle cells in Col-0 displaying high lobeyness and normal growth. (**B, F**) Thin and elongated epidermal pavement cells in the

CA-ROP2 mutant displaying decreased lobeyness (**B**), with long and thin leaves, and reduced overall plant growth (**F**). (**C, G**) Snaky epidermal pavement cells in the *any1* mutant displaying decreased lobeyness (**C**), with smaller and round leaves, and dwarf plant phenotypes (**G**). (**D, H**) Small epidermal pavement cells in the *ctr1* mutant displaying decreased lobeyness (**D**), with very small leaves, and dwarf plant phenotypes (**H**). (**I-Q**) The effect of pharmacological treatments on the shape of epidermal pavement cells. (**I**) The mock treatment (DMSO) retains the typical morphology of puzzle cells. (**J-M**) Dose-dependent oryzalin treatments result in a gradual decrease in lobeyness and an increase in LEC (cells labelled in violet). (**N-Q**) Dose-dependent latrunculin B treatments lead to a decrease in lobeyness with shallow lobes (cells labelled in yellow). (**R**) Treatments were administered at increasing concentrations of 0.5, 1, 5 and 8 μM. The 95th percentile of lobeyness is plotted for each drug treatment, with statistical significance determined using bootstrapping by pairwise comparisons to DMSO; significance is marked by asterisks and standard error. (**S**) The 95th percentile of lobeyness for different mutants, with statistical significance determined using bootstrapping by pairwise comparisons to Col-0; significance is marked by asterisks and standard errors. Scale bars: (contours **I-Q**) 50 μm, (epidermis **I-Q**) 100 μm, (**A-D**) 200 μm, (**H**) 1 mm, (**G**) 2 mm, (**F**) 5 mm, (**E**) 50 mm.

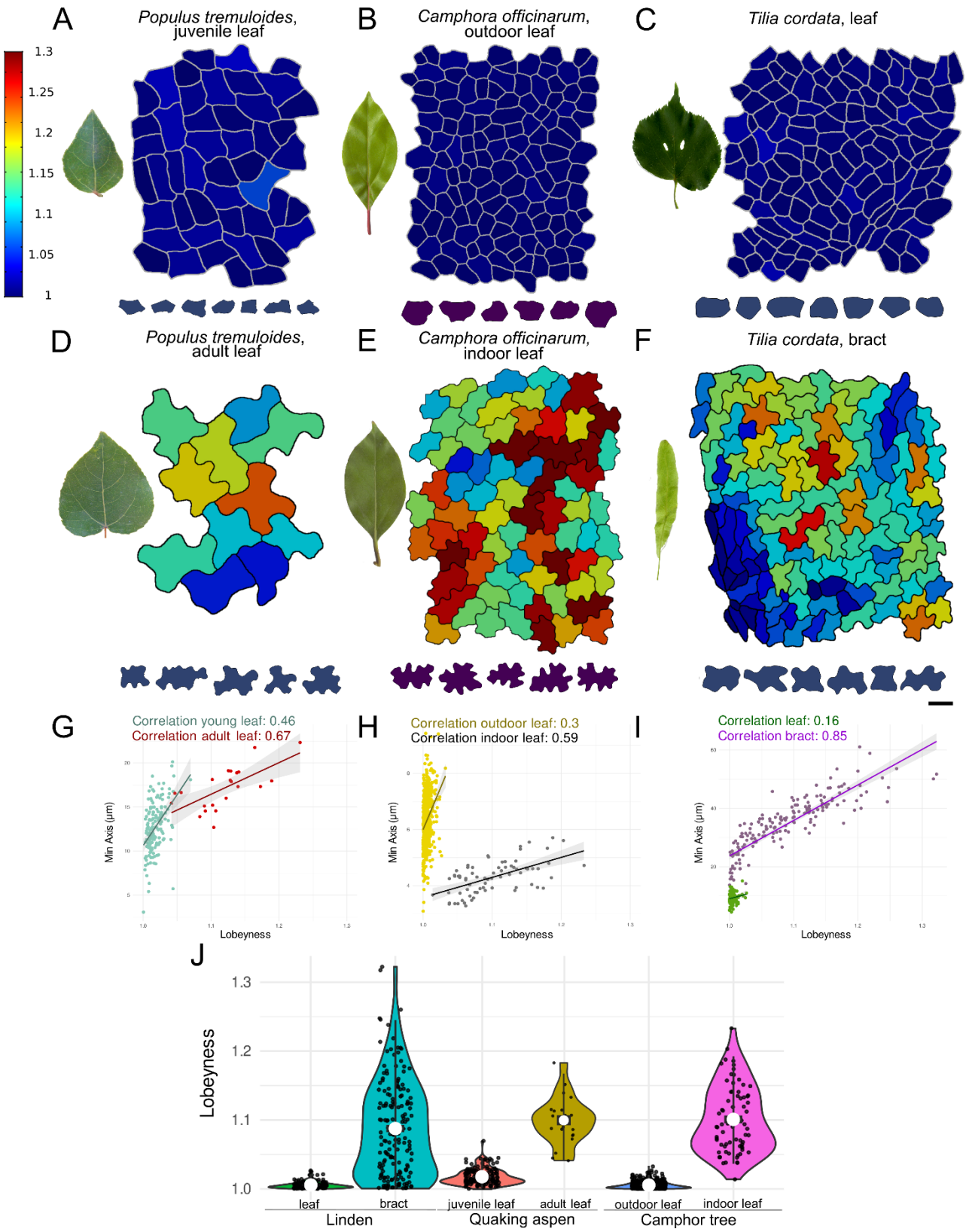

Figure 4. Pavement cell shapes exhibit developmental and environmental plasticity, varying across organs. (**A-F**) Leaf photographs are paired with lobeyness heatmaps of pavement cell contours and outlines near the 95th percentile of lobeyness. (**A**, **D**) Quaking aspen (*Populus tremuloides*), showing juvenile (**A**) and adult (**D**) leaves on the adaxial surface. (**B**, **E**) Camphor tree (*Camphora officinarum*) leaves grown outdoors (**B**) and indoors (**E**). (**C**, **F**) Linden (*Tilia cordata*) leaves (**C**) and bracts (**F**). (**G-I**) Scatter plots of the correlation between lobeyness and min-axis (the shortest cell dimension): (**G**) quaking aspen juvenile (Corr = 0.46) vs adult (Corr = 0.67) leaves, (**H**) camphor tree outdoor (Corr = 0.3) vs indoor (Corr = 0.59) leaves, and (**I**) linden leaf (Corr = 0.16) vs bract (Corr = 0.85). (**J**) Violin plots showing

lobeyness distributions under each condition or organ, with the median indicated by a white circle, the interquartile range by a black box, and whiskers at 1.5 times the interquartile range. Scale bar: (**D** heatmap**, E** heatmap) 10 μm, (**A** heatmap) 15 μm, (**B, C, D** contours) 20 μm, (**B** heatmap, **E** contours) 25 μm, (**C** heatmap) 40 μm, (**F** heatmap**,** contours) 50 μm.

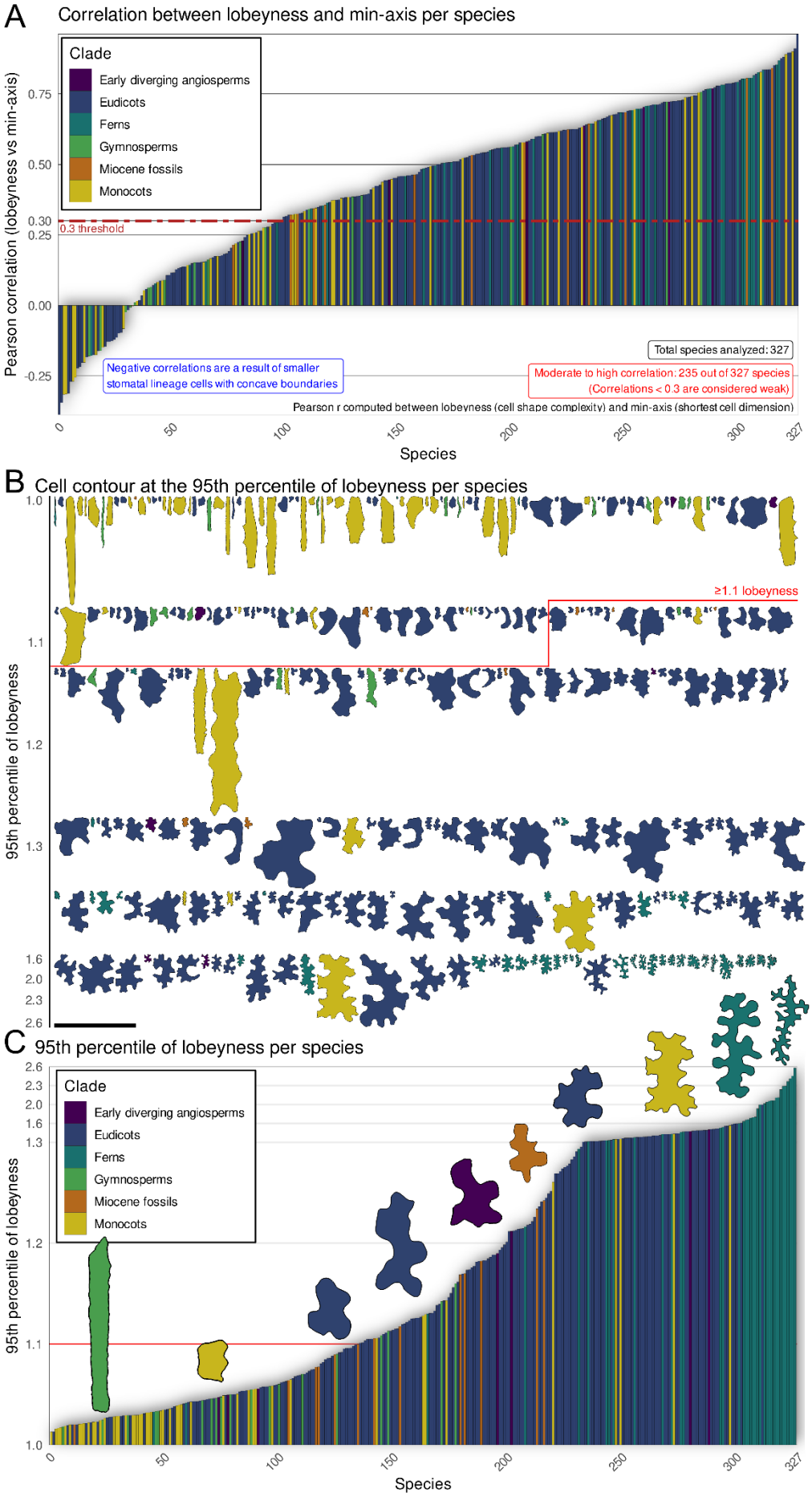
A
Correlation between lobeyness and min-axis per species
Clade
Early diverging angiosperms
Eudicots
Ferns
Gymnosperms
Miocene fossils
Monocots
Pearson correlation (lobeyness vs min-axis)
0.75
0.50
0.30
0.25
0.00
-0.25
0.3 threshold
Total species analyzed: 327
Negative correlations are a result of smaller stomatal lineage cells with concave boundaries
Moderate to high correlation: 235 out of 327 species
(Correlations < 0.3 are considered weak)
Pearson r computed between lobeyness (cell shape complexity) and min-axis (shortest cell dimension)
0
50
100
150
200
250
300
327
Species
B
Cell contour at the 95th percentile of lobeyness per species
95th percentile of lobeyness
1.0
1.1
1.2
1.3
1.6
2.0
2.3
2.6
≥1.1 lobeyness
C
95th percentile of lobeyness per species
Clade
Early diverging angiosperms
Eudicots
Ferns
Gymnosperms
Miocene fossils
Monocots
95th percentile of lobeyness
2.6
2.3
2.0
1.6
1.3
1.2
1.1
1.0
0
50
100
150
200
250
300
327
Species

Figure 5. Lobeyness is a common feature observed across different species. (A) Bar plot displaying the Pearson correlation (r) computed between lobeyness (cell shape complexity) and min-axis (the shortest cell dimension) across 327 species. Correlations below 0.3 are deemed weak while those at or above 0.3 are classified as moderate to high. In our analysis, 235 out of 327 species exhibited moderate to high correlations. The 0.3 threshold was selected as a heuristic cutoff to differentiate species with pronounced positive relationships from those with less pronounced associations. Bars are color-coded by clade. (**B**) Visual representation of a single pavement cell contour per species, selected at the 95th percentile of lobeyness. The contours are arranged in order of increasing cell shape complexity, color-coded by clade. The 1.1 threshold was selected as a heuristic cutoff to differentiate species with significant lobeyness from those with less pronounced lobes. (**C**) Bar plot of the 95th percentile of lobeyness values with selected cell contours superimposed. The contours are color-coded by clade. The contours at approximate lobeyness values 1 (mountain cypress, *Widdringtonia nodiflora*), 1.05 (Panama hat plant, *Carludovica palmata*), 1.1 (yellow trumpetbush, *Tecoma stans*), 1.15 (garlic mustard, *Alliaria petiolata*), 1.2 (Japanese star anise, *Illicium anisatum*), 1.25 (colicwood, *Myrsine*), 1.3 (yarrow, *Achillea millefolium*), 1.5 (Peruvian lily, *Alstroemeria aurea*), 2 (*Phanerophlebia*), and 2.5 (rough maidenhair fern, *Adiantum hispidulum*) were selected to represent all clades at increasing positions along the lobeyness gradient (minimum 1.0 to maximum 2.6). Emphasis is given to the range from 1.0 to 1.3, as significant lobeyness begin to appear around a lobeyness value of 1.1. Scale bars: (**C** contours lobeyness values 1, 1.05, 1.15, 1.25, 1.3, 2, 2.5) 100 µm, (**C** contours lobeyness values 1.1, 1.2) 200 µm, (**C** contours lobeyness value 1.5) 400 µm, (**B**) 500 µm.